0013-7227/05/$15.00/0
Printed in U.S.A.

Endocrinology 146(11):4584–4596

doi: 10.1210/en.2005-0333

Cells of the Osteoclast Lineage as Mediators of the Anabolic Actions of Parathyroid Hormone in Bone

Amy J. Koh, Burak Demiralp, Kathleen G. Neiva, Joanna Hooten, Rahime M. Nohutcu, Hyunsuk Shim, Nabanita S. Datta, Russell S. Taichman, and Laurie K. McCauley

Department of Periodontics and Oral Medicine, School of Dentistry (A.J.K., J.H., N.S.D., R.S.T., L.K.M.), Oral Health Sciences Ph.D. Program, School of Dentistry (K.G.N.), and Department of Pathology, Medical School (L.K.M.), University of Michigan, Ann Arbor, Michigan 48109; Winship Cancer Institute (H.S.), Emory University, Atlanta, Georgia 30322; and Department of Periodontology, Faculty of Dentistry (B.D., R.M.N.), Hacettepe University, Ankara 06100, Turkey

PTH is an anabolic agent used to treat osteoporosis, but its mechanisms of action are unclear. This study elucidated target cells and mechanisms for anabolic actions of PTH in mice during bone growth. Mice with c-*fos* ablation are osteopetrotic and lack an anabolic response to PTH. In this study, there were no alterations in PTH-regulated osteoblast differentiation or proliferation *in vitro* in cells from c-*fos* −/− mice compared with +/+; hence, the impact of osteoclastic cells was further investigated. A novel transplant model was used to rescue the osteopetrotic defect of c-*fos* ablation. Vertebral bodies (vossicles) from c-*fos* −/− and +/+ mice were implanted into athymic hosts, and the c-*fos* −/− osteoclast defect was rescued. PTH treatment to vossicle-bearing mice increased 5-bromo-2′-deoxyuridine (BrdU) positivity in the bone marrow and increased bone area regardless of the vossicle genotype. To inhibit recruitment of osteoclast precursors to wild-type vossicles, stromal derived factor-1 signaling was blocked, which blunted the PTH anabolic response. Treating mice with osteoprotegerin to inhibit osteoclast differentiation also blocked the anabolic action of PTH. In contrast, using c-*src* mutant mice with a late osteoclast differentiation defect did not hinder the anabolic action, suggesting key target cells reside in the intermediately differentiated osteoclast population in the bone marrow. These results indicate that c-*fos* in osteoblasts is not critical for PTH action but that cells of the osteoclast lineage are intermediate targets for the anabolic action of PTH. (*Endocrinology* 146: 4584–4596, 2005)

BONE IS A SPECIALIZED and dynamic tissue that undergoes continuous remodeling throughout life. Osteoblasts are the cells responsible for the synthesis and mineralization of the bone matrix and hence have been considered the primary targets for the actions of PTH in bone. PTH has both anabolic and catabolic actions in bone, but recent interest has increased the focus on anabolic actions of PTH due to its therapeutic potential. PTH, currently marketed as FORTEO in the United States for the treatment of postmenopausal osteoporosis, results in an increase in vertebral, femoral, and total-body bone mineral density (1). Although it has been reported that the anabolic actions of PTH are dependent on an intermittent regimen, the N-terminal peptide of PTH (2), cAMP stimulation (3), inhibition of apoptosis (4), and Runx2 (5), the complete picture of PTH action is still unclear. Interestingly, recent clinical studies and an animal study found that a bisphosphonate was capable of blunting the anabolic response to PTH, suggesting that active bone remodeling may be critical for anabolic actions of PTH (6–8). These studies highlight the importance of understanding the mechanisms of PTH action to optimize therapeutic regimens and combinatorial approaches to treat bone disorders.

PTH often has differing effects *in vitro* compared with the *in vivo* setting, but one transcriptional mediator that is increased rapidly upon PTH administration *in vivo* and *in vitro* is c-*fos* (9, 10). The protooncogene c-*fos* is the cellular homologue of v-*fos*, which was identified originally in the Finkel, Biskis, Jinkins (FBJ-) and Finkel, Biskis, Reilly (FBR-) murine sarcoma viruses (11). The immediate early gene c-*fos* is a member of the activator protein-1 (AP-1) transcription factor complex. AP-1 is formed by Fos-related (c-Fos, FosB, Fra-1, and Fra-2) and Jun-related (c-Jun, JunB, and JunD) proteins. Inactivation of c-*fos* causes the bone remodeling disease osteopetrosis, which is characterized by impaired osteoclastic bone resorption, resulting in a net increase in skeletal mass (12). Mice lacking c-*fos* have a profound osteoclast defect demonstrating that c-*fos* is a critical transcriptional mediator of osteoclast differentiation (12, 13). In contrast, when c-*fos* is overexpressed in tissues, bone tumors develop that are typically chondroblastic osteosarcomas, characterized by large amounts of neoplastic bone with foci of cartilage (14). It is thought that the mechanisms regulating the number of osteoblasts can be controlled, at least in part, by Fos and AP-1 (15). The protooncogene c-*fos* is important in endochondral ossification; however, studies with c-*fos*-deficient mice indicate that c-*fos* is not necessary for the differentiation of osteoblasts (16, 17). Studies from our laboratory demonstrated that mice with an ablation of the c-*fos* gene did not respond to PTH in an anabolic manner but instead displayed an antianabolic response to PTH *vs.* wild-type mice during a

First Published Online August 4, 2005

Abbreviations: AP-1, Activator protein-1; BrdU, 5-bromo-2′-deoxyuridine; CXCR4, Cys-X-Cys chemokine receptor 4; DTT, dithiothreitol; OPG, osteoprotegerin; RANK, receptor activator of nuclear factor κB; RANKL, RANK ligand; SDF-1, stromal derived factor-1; SSC, standard saline citrate; TRAP, tartrate acid phosphatase.

***Endocrinology* is published monthly by The Endocrine Society (http://www.endo-society.org), the foremost professional society serving the endocrine community.**

period of endochondral bone growth (18). This work substantiated a critical role for c-*fos* in the anabolic actions of PTH. However, it is unclear whether this is a direct effect of PTH on osteoblastic activity or an indirect effect associated with the lack of osteoclasts in these mutant mice. Elucidation of this selective modification of c-*fos* on the anabolic actions of PTH will provide valuable insights into the actions of PTH and its therapeutic optimization, *e.g.* via combinatorial approaches, for the treatment of skeletal deficiencies as in osteoporosis or skeletal fractures. The goals of this study were to examine the role of c-*fos* in PTH effects on osteoblast proliferation, differentiation, and gene expression and also to examine the role of osteoclasts as indirect mediators of the anabolic actions of PTH in bone.

Materials and Methods

Murine models

All animals were maintained in accordance with institutional animal care and use guidelines and experimental protocols approved by the Institutional Animal Care and Use Committee of the University of Michigan. Mice (B6/129) heterozygous for the *Fos*^{tm1Pa} deletion mutation were obtained from The Jackson Laboratory (Bar Harbor, ME). Neonatal mouse pups were typed at birth to distinguish homozygous, heterozygous, and wild-type mice. A PCR protocol using two sets of two primers was used as described (17). Primers 022 (5′-CAA CGC CGA CTA CGA GGC GTC AT-3′) and 023 (5′-CAA GTG TGC ACG CGC TCA GAC AA-3′) amplify a 299-bp endogenous band from *Fos*, primer 009 (5′-TAA AAC GCA CGG GTG TTG GGT-3′) and primer 024 (5′-CCC CTG CGA GTC ACA CCC CAG-3′) amplify a 190-bp band from the junction fragment of neo and *Fos*. Standard PCR protocols were performed as described (17). Mice (B6/129) heterozygous for the *Src*^{tm1Sor} targeted mutation were also purchased from The Jackson Laboratory. A PCR protocol based on the previously published characterization of these mice was used (19). Primers E2 (5′-AGC AAC AAG AGC AAG CCC AAG GAC-3′) and E2–3 (5′-GTG ACG GTG TCC GAG GAG TTG AAG-3′) amplify a 200-bp wild-type band from *c-src*. Primers E2–3 and 9603 (5′-TCA TAG CCG AAT AGC CTC TCC AC-3′) amplify a 350-bp mutant band. Phenotypes of homozygous mutants of both strains were also confirmed by lack of tooth eruption. Breeding colonies were established using heterozygote mice to provide litter mate controls. Luciferase-expressing mice were kindly provided by Dr. Kurt Hankenson (University of Michigan, Ann Arbor, MI) and have been described (20). These transgenic reporter mice have luciferase expression driven by the nuclear factor κB-dependent portion of the HIV-1 long terminal repeat and widely express luciferase upon injection of its luciferin substrate as we have described in another model system (21).

In vivo treatment protocols

Mice were administered hPTH(1–34) (Bachem, Torrence, CA) or vehicle (0.9% saline) by sc injection at 50 μg/kg·d or 80 μg/kg·d for indicated time periods. In selected experiments, osteoprotegerin (OPG) (R&D Systems, Minneapolis, MN) was administered at 4 mg/kg twice a week for the first 2 wk either alone or in combination with PTH. For the stromal derived factor-1 (SDF-1) studies, mice were administered a mixture of a Cys-X-Cys chemokine receptor 4 (CXCR4) blocking peptide designed to inhibit SDF-1 binding to the CXCR4 (TN14003; NH_2-RR-Nal-CY-Cit-K-$_D$K-PYR-Cit-CR-amide, 1 μg/d) synthesized by the Emory Microchemical Facility (22) and antihuman/mouse SDF-1 IgG antibody [pre-B-cell growth-stimulating factor/SDF-1 monoclonal antibody (clone 79014), 25 μg/d, R&D Systems] administered ip daily in 100 μl PBS. Controls were injected with a similar mixture of a control peptide and IgG antibody, where the control peptide was produced by randomly scrambling the amino acid sequence of CXCR4 antagonist while maintaining the disulfide bond to maintain the U-type structure of the antagonist (NH_2-KY-Nal-YR-$_D$K-Cit-RCRRP-Cit-C-amide) (23). The peptide has been validated to inhibit cancer cell migration to SDF-1, inhibit SDF-1 binding to prostate cancer cells, and inhibit breast cancer metastasis in mice (23, 24). In a previous study, we found that a 4-wk administration of this peptide significantly reduced serum tartrate acid phosphatase (TRAP)5b levels (vehicle, 1.51 ± 0.10 U/liter; anti-CXCR4 peptide, 1.12 ± 0.10 U/liter; $P < 0.05$) and osteoclastic activity in the bones of mice (24).

Isolation of primary calvarial cells and cell culture

Primary calvarial cells were isolated as previously described (25). Briefly, calvariae of mice (11–15 d old) were dissected, isolated from periosteum, and subjected to sequential digestions of 20, 40, and 90 min in collagenase A (2 mg/ml, Roche Molecular Biochemicals, Indianapolis, IN) with 0.25% trypsin (Invitrogen, San Diego, CA). Cells from the third digestion were washed, counted, and plated in α-MEM with 10% fetal bovine serum containing 100 U/ml penicillin and 100 mg/ml streptomycin, at different densities according to the assays. Medium was changed every other day. Primary cultures were used without passage for proliferation and mineralization assays, whereas cultures at the first passage were used for gene expression assays.

Cell enumeration and apoptosis

Primary osteoblasts isolated from calvariae were plated in 24-well plates at a density of 5000 cells/cm^2. Cells were treated with 0.1 μM PTH(1–34) or vehicle (HCl/BSA) every other day for 0–8 d. Cells were enumerated using a hemocytometer at d 0, 4, 6, and 8 and cell viability determined by trypan blue dye exclusion.

The Cell Death Detection ELISA Plus Kit (Roche Molecular Biochemicals), a quantitative sandwich enzyme immunoassay, was used to measure histone-complexed DNA fragments for apoptosis detection. Primary osteoblastic cells were plated in 24-well plates at a density of 5000 cells/cm^2, and medium was changed every other day. The apoptosis ELISA was performed at d 6 and 7. Etoposide (100 μM) for 36 h was used as a positive control. Cell lysates were added to each well in a streptavidin-coated microplate and a mixture of antihistone-biotin and anti-DNA-peroxidase was added for 2 h. After incubation with 2.2′-azino-di[3-ethyl-benz-thiazolin-sulfonate] substrate, peroxidase was measured at 405 nm against a 2.2′-azino-di[3-ethyl-benz-thiazolin-sulfonate] blank (reference wavelength at 490 nm). Cells were also enumerated using a hemocytometer at d 8, and cell viability was determined by trypan blue dye exclusion.

SDS-PAGE and Western analysis

Western analysis was performed as described (26). Briefly, cells were washed twice with cold PBS, lysed for 30 min at 4 C after sonication with radioimmunoprecipitation assay buffer containing protease inhibitors (Sigma, St. Louis, MO), and cleared by centrifugation. An aliquot of each lysate was removed for protein concentration determination. SDS-PAGE was performed in 10–12% polyacrylamide gels. Each lane contained between 40–80 μg of cell (lysate) protein. Prestained molecular weight standards were run in parallel lanes. After electrophoresis, the proteins were transferred to polyvinylidene difluoride membrane (Bio-Rad Laboratories, Inc., Hercules, CA) in buffer containing 25 mM Tris-HCL, 192 mM glycine, 20% vol/vol methanol, and 0.01% sodium dodecyl sulfate (pH 8.5). Residual protein binding sites on the membrane were blocked by incubation for 3 h to overnight in Tris-buffered saline with Tween 20 buffer [20 mM Tris-HCL (pH 7.6), 137 mM NaCl, and 0.5% Tween 20] containing 5% nonfat dry milk. The membranes were incubated with the primary antibody for 2 h to overnight. After washing with Tris-buffered saline with Tween 20, the secondary antibody (anti-IgG conjugated with horseradish peroxidase) was added and incubated for 20–30 min. Finally the proteins were visualized by autoradiography using an enhanced chemiluminescence detection system (Pierce, Rockford, IL).

von Kossa staining and calcium content of cultures

Cells from c-*fos* genotypes were treated with mineralization media (ascorbic acid, 50 μg/ml and β-glycerophosphate, 10 mM) and hPTH(1–34) (0.1 μM) or vehicle (HCl/BSA) for 24 d. At the end of the culture period, cells were fixed with 95% EtOH and stained with $AgNO_3$ using the von Kossa method to detect phosphate deposits in bone nodules as described (25). For calcium accumulation, cultures from c-*fos* genotypes

were treated with mineralization media and vehicle or hPTH(1–34) (0.1 μM) every other day for 14 d. Calcium accumulation in cell layers was determined after extraction with 15% trichloroacetic acid followed by colorimetric determination via cresolphthalein complexone (Sigma). DNA was quantified using a fluorometer as described (27).

Northern blot analysis

Total RNA was isolated using the guanidinium isothiocyanate method and quantified by spectrophotometry as described (10). Total RNA (10 μg) was electrophoresed on 1.2% agarose-formaldehyde gels. The RNA was transferred to nylon membranes (Duralon U.V., Stratagene, La Jolla, CA) and UV cross-linked. The nylon membranes were hybridized with a cDNA probe encoding IL-6 or IGF-1. After hybridization and washing, radioactive counts per minute were quantified using an Instant Imager (Packard Instrument Co., San Diego, CA). The blots were then exposed to Kodak X-OMAT film at −70 C for 24–72 h to obtain band images. Blots were also stripped and reprobed with a cDNA probe for 18S rRNA to control for RNA loading.

Bone implants and histomorphometry

Lumbar vertebrae were sterile isolated from c-*fos* or c-*c-src* mutant, heterozygote, and wild-type mice 4 d after birth. Soft tissues were dissected, and vertebrae were sectioned into single vertebral bodies (vossicles) with a scalpel blade. Subsets of vossicles were microradiographed, fixed in formalin, and decalcified in 10% EDTA (pH 7.4) for 7 d as baseline samples. Athymic (nude) mice (4–6 wk) (Harlan, Indianapolis, IN) were used as transplant recipients. After anesthesia [ip injection of a ketamine (90 mg/kg) and xylazine (5 mg/kg) cocktail], vossicles (four to six per mouse) were washed with Hanks' balanced salt solution and implanted into sc pouches. Briefly, 1-cm incisions were made along the backs of mice. Pouches were made on either side of the incision with blunt dissection and vossicles implanted. The next day, hPTH or vehicle, or in selected experiments OPG- or SDF-1-blocking peptides, were administered as described above and continued for 3 wk. Two hours before the mice were killed, 5-bromo-2′-deoxyuridine (BrdU) labeling reagent (Zymed, South San Francisco, CA) was administered ip at a dose of 10 μl/g. At the time the mice were killed, vossicles were exposed to x-ray film (GREEN, Wolverine X-Ray, Dearborn, MI) at 4×, 32 kV, 15 sec in a FAXITRON x-ray machine (FAXITRON, Madison, WI) fixed in formalin overnight, then demineralized in 10% EDTA (pH 7.4) for 7 d. Tissues were paraffin embedded, sectioned, stained for hematoxylin and eosin (H&E), and histomorphometry was performed.

Histological assays

Histomorphometric analysis was performed as previously described (18, 28). Briefly, paraffin-embedded vossicles and vertebrae were cut at 5 μm, stained with H&E, and total bone area measured using a computer-assisted bone histomorphometric analyzing system (Image-Pro Plus version 4.0, Media Cybernetics, Inc., Silver Spring, MD). TRAP staining was performed using a leukocyte acid phosphatase assay from Sigma Diagnostics and data expressed as numbers of osteoclasts per millimeter of bone. BrdU staining was performed using the BrdU Staining Kit from Zymed Laboratories per the manufacturer's protocol. Briefly, vossicles were dewaxed, hydrated, and quenched with 3% H_2O_2 for 10 min. Sections were trypsinized for 10 min, then denatured for 30 min at room temperature. After 10 min of blocking, sections were incubated with biotinylated anti-BrdU for 1 h at room temperature, then with streptavidin-peroxidase for 10 min. Sections were stained brown with diaminobenzidine and counterstained with hematoxylin. After dehydration and clearing, slides were mounted with Histomount and coverslipped. Rabbit antiluciferase antibody (1:3200, Sigma) with EnVision Rabbit Peroxidase Kit (Dako Corp., Capinteria, CA) was used for luciferase immunohistochemistry. Digoxin *in situ* hybridization was performed for SDF-1 detection in normal murine tibiae from mice treated with PTH (80 μg/kg) or vehicle for 3 wk. Paraffin sections were treated with proteinase K, 10% formalin, and washed in standard saline citrate (SSC). Hybridization was performed with digoxin-labeled SDF-1 sense or antisense riboprobes at 55 C overnight. After incubation, the slides were washed in 4× SSC, Rnase A, 2× SSC-10 mM dithiothreitol (DTT), 1× SSC-10 mM DTT, and 0.5× SSC-10 mM DTT. The slides were then washed, blocked in 2% blocking buffer for 1 h, 1:500 antibody, and color developed using nitro blue tetrazolium and 5-bromo-4-chloro-3-indolyl phosphate.

Statistical analysis

All *in vitro* experiments were performed at least three times with similar results and representative assay shown. *In vivo* experiments were performed with the indicated number of replicates per group. Statistical analysis was performed by ANOVA or Student's *t* test using the GraphPad Instat statistical program with significance at $P < 0.05$.

Results

Proliferation assays

Adherence of cells to plates was similar in all genotypes as evidenced by similar cell counts at d 0 (~20 h after plating) among all c-*fos* genotypes (Fig. 1A). By d 4, there was a slight increase in the number of cells from c-*fos* −/− mice, and cells from all genotypes became confluent at d 5 or 6. The difference between genotypes was greater at d 6 but was only significant between c-*fos* −/− and c-*fos* +/− ($P < 0.05$). After confluence, at d 8, the numbers of cells from c-*fos* −/− mice were higher than both c-*fos* +/− ($P < 0.05$) and +/+ ($P < 0.01$). There was no significant difference between c-*fos* +/+ and +/− cell cultures at any time point. PTH(1–34) treatment did not alter the cell number of cultures from any genotype at any time point (Fig. 1B). Similar to vehicle-treated cells, the PTH-treated c-*fos* −/− osteoblast cultures had increased numbers of cells compared with c-*fos* +/+ cultures at d 8 ($P < 0.05$). These data suggest that the c-*fos* −/− cells have a growth advantage after confluence but that there is no alteration in the response to PTH for any genotype.

Apoptosis

To assess the role of apoptosis in the increased cell number of cultures from c-*fos* mutant mice, an apoptosis ELISA was performed. Apoptosis was measured at d 6 and 7 because the cell enumeration assays revealed differences from d 6–8. Cell enumeration assays were performed at d 8 to validate the difference in cell numbers among the genotypes and to determine whether etoposide altered the effect. There were no differences in apoptotic cell indices between the genotypes at either d 6 or 7 (Fig. 1C). Etoposide treatment increased the apoptotic cell indices in both groups on both days ($P < 0.05$). At d 8, c-*fos* −/− cultures had higher numbers of viable cells *vs.* c-*fos* +/+ ($P < 0.005$), but both groups were reduced in number with etoposide treatment to a similar extent. These data suggest that the increase in cell number of the c-*fos* mutant mice was not due to a protection from apoptosis.

Cell cycle protein expression

To validate a proliferative advantage for the increase in cell numbers in the c-*fos* mutant mice, analysis of cyclin D1 was performed. Cyclin D1 is a cell cycle progression factor at the G_1 phase, and we have reported that it is reduced in response to PTHrP treatment (29). The c-*fos* mutant mice had increased levels of cyclin D1 (Fig. 1, D and E). Treatment with PTHrP reduced cyclin D1 levels similarly in c-*fos* +/+ and −/− cultures. This result suggests that the c-*fos* mutant mice have

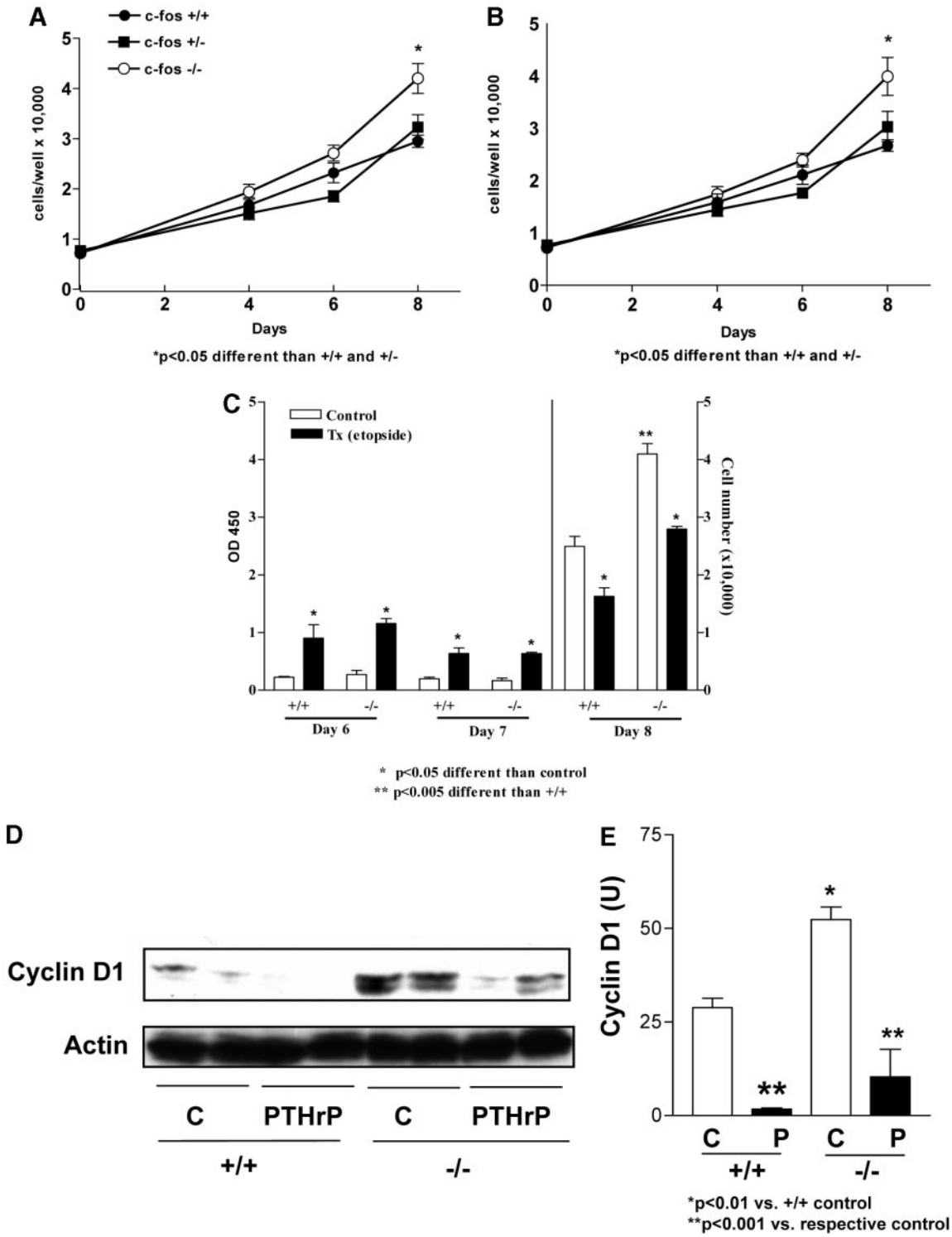

FIG. 1. Role of c-*fos* in osteoblastic cell proliferation/apoptosis. A, c-*fos* cell enumeration over time. Cells were plated at 5000/well and at d 0 (20 h after plating), 4, 6, and 8, cells were trypsinized and counted via trypan blue dye exclusion. The cells from all genotypes increased in number from d 1–8, but cells with ablation of the c-*fos* gene (−/−) had greater numbers at d 8 compared with +/+ and +/−. B, Cultures were performed as in A, but PTH was added to culture media every 2 d (treatment groups are the same as for A but in the presence of PTH). PTH did not alter the cell numbers, and c-*fos* mutant cultures still had greater numbers of cells at d 8 *vs.* +/+ and +/−. C, For apoptosis detection, primary osteoblastic cells were plated at 5000 cells/cm^2, and apoptosis was detected by a DNA fragmentation ELISA performed at d 6 and 7 (*left*) or trypan blue dye exclusion cell enumeration (*right*). Etoposide (100 μM) for 36 h was used to stimulate apoptosis. Etoposide increased DNA fragmentation at d 6 and 7 and reduced cell numbers at d 8, but there was no difference between cells from the +/+ or −/− genotypes. D and E, Western blot analysis of the G_1 phase cyclin D1. Primary osteoblasts from c-*fos* +/+ or −/− mice were treated with control or PTHrP (10 nM) for 5 h. Cell lysates were collected, and Western blot analysis for cyclin D1 was performed. Cyclin D1 levels were higher in cultures from −/− mice. Cells from both genotypes had similarly reduced cyclin D1 protein with PTHrP treatment.

a proliferative advantage through alteration of cell cycle proteins but that there is no alteration in their PTH-mediated response.

Calcium incorporation and von Kossa staining

To assess the role of c-*fos* in osteoblast differentiation, calcium incorporation and mineralized nodule formation were evaluated *in vitro*. There were no qualitative differences in nodule formation visualized by von Kossa staining (Fig. 2A). PTH(1–34) treatment decreased mineralized nodule formation, as we have previously reported (25), in cell cultures from all genotypes. This suggests that the direct effect of PTH on differentiating osteoblasts is an inhibitory one. Although there was a trend of more calcium accumulation in mineralizing cultures from c-*fos* −/− mice, there were no significant differences in the amount of calcium incorporation between the genotypes (Fig. 2B). PTH(1–34) treatment decreased the calcium accumulation similarly in cell cultures from all genotypes. The trend in increased calcium accumulation may be associated with the increased proliferative effect postconfluence but that there was no significant difference among cultures indicates that there was no alteration in differentiation. More importantly, there was no difference in the PTH response to inhibit osteoblast differentiation among groups.

Northern blot analysis

To evaluate whether c-*fos* is critical for PTH(1–34) actions on downstream genes important in bone metabolism, Northern blot analysis was performed. IL-6, a proresorptive cytokine, and IGF-1, a proformation growth factor, were evaluated. PTH(1–34) induced similar temporal mRNA expression for IL-6 and IGF-1 in cells from +/+, +/− (data not shown), and −/− mice (Fig. 2, C and D). IGF-1 mRNA expression levels increased with 3 h of PTH(1–34) treatment and declined thereafter but were detectable at all time points. Two IGF-1 bands were detected, and the stronger band quantified and plotted in Fig. 2D. IL-6 mRNA was strongly detected at 1 and 3 h after PTH administration in all genotypes and declined thereafter. These data further support the lack of a

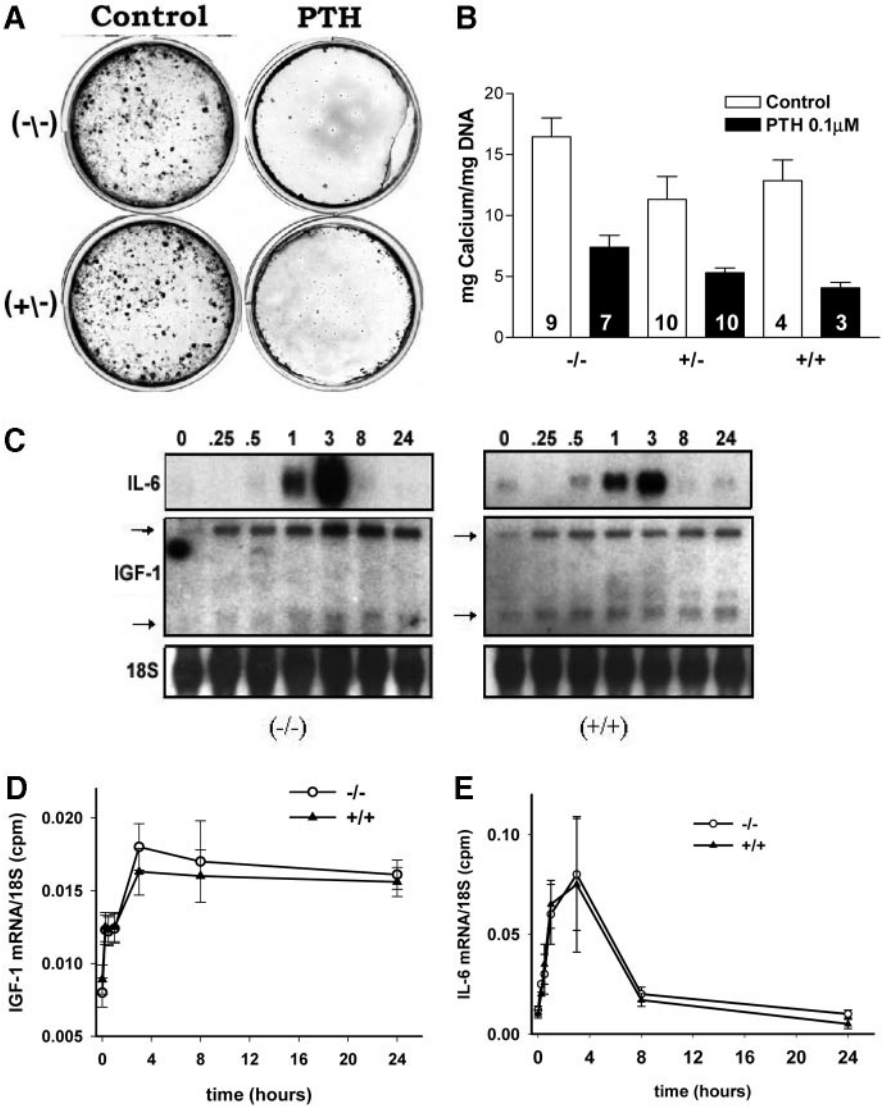

FIG. 2. Role of c-*fos* in osteoblastic cell differentiation. A, von Kossa-stained plates. Primary calvarial osteoblasts were cultured from c-*fos* +/+, +/−, and −/− mice and induced to differentiate with or without PTH (0.1 μM) for 21 d. von Kossa staining of phosphate deposits demonstrates similar bone nodule formation in +/− and −/− cultures where PTH was capable of reducing nodule formation in both groups (+/+ was similar to +/−; data not shown). B, Calcium detection was performed on cultures as described in A. There was no difference in the amount of calcium expressed per milligram of DNA for any of the genotypes, and PTH reduced incorporation similarly among cells from the various genotypes (n values indicated on *bars*). C, Representative Northern blot analysis of primary osteoblastic cells from c-*fos* −/− (*left*) or +/+ (*right*) mice treated with PTH (0.1 μM) for the designated time periods (hours). D, Graphic representation of data from multiple northern analyses (n = 3/group). There was an increase in IGF-1 mRNA (*left*) and IL-6 mRNA (*right*) in response to PTH but no difference in expression in cells from +/+ or −/− mice.

direct effect of PTH on c-*fos* mutant osteoblasts that differs from wild-type mice.

Vossicle model system

We have previously characterized an ectopic ossicle model system that responds to PTH with an anabolic result that is greater than endogenous bone (28, 30). The principle of this model system was used to separate out the mesenchymal and hematopoietic components of the bone and elucidate the target of the PTH-altered response in the c-*fos* −/− mutant mice. Figure 3A demonstrates the model system as described in *Materials and Methods*. Vertebral bodies from 4-d-old c-*fos* +/+ mice (Fig. 3B) at baseline (preimplantation) demonstrate early formation of trabecular bone and a hematopoietic marrow cavity, whereas vertebral bodies from 4-d-old c-*fos* −/− mice have a minimal marrow cavity (Fig. 3C). However, after implantation and PTH treatment, the c-*fos* −/− implants recruit a hematopoietic marrow and numerous TRAP+ osteoclastic cells from the host tissues (Fig. 3D). To validate the mesenchymal contribution of this model, we implanted vertebral bodies from mice expressing luciferase under the HIV1 long terminal repeat promoter. *In vivo* imaging confirmed the expression of luciferase in the vossicle implants (Fig. 3E). At the time the mice were killed, immunohistochemistry for luciferase was performed as described (21). Figure 3F demonstrates that osteoblastic cells lining the vossicle trabeculae in a PTH-treated (3 wk) mouse are luciferase positive and hence derived from the donor, not via rescue from the host.

Vossicles from c-*fos* +/+ and −/− mice after 21 d of implantation appeared similar in size and organization (Fig. 4A). Both genotypes displayed cortical and trabecular bone and a hematopoietic marrow. PTH treatment increased the bone area of implants from both genotypes to a similar extent (Fig. 4B). This substantiates that c-*fos* expression in the mesenchymal compartment is dispensable for the anabolic actions of PTH. TRAP staining was performed to determine the numbers of osteoclasts present in vossicles (Fig. 4C). Although there was a trend for greater osteoclast numbers in the c-*fos* −/− bones, there was no difference between groups at this end point. Finally, BrdU staining demonstrated an altered pattern of positivity in vossicles treated with PTH (Fig. 4D). Vehicle-treated vossicles (c-*fos* +/+ or −/−) displayed BrdU positivity that tended to be restricted to the cells

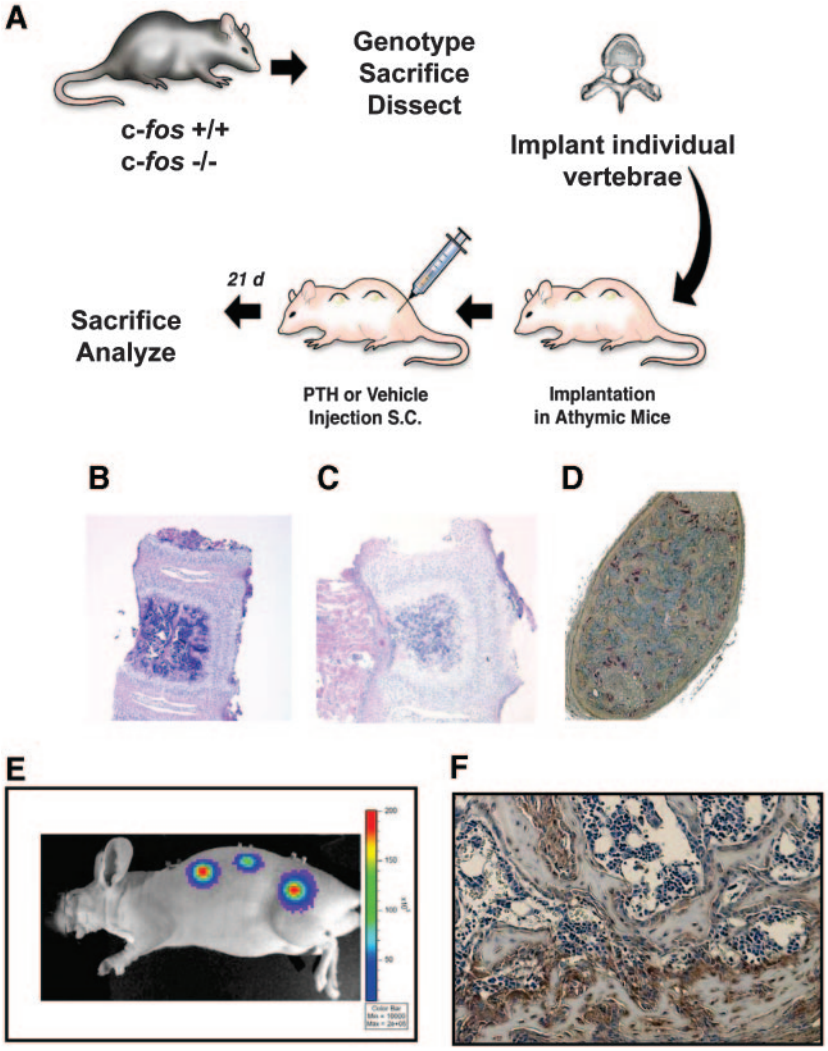

FIG. 3. A, Vossicle implant experimental design. Vertebrae from neonatal (d 4) mice of various genotypes were dissected, trimmed of musculature, and implanted into athymic hosts. PTH or vehicle was administered via sc injection for 3 wk before the mice were killed. B and C, Histologic view of vossicles at baseline (vertebrae from neonatal d 4 mice dissected and ready for implantation). Vertebra from a c-*fos* +/+ (B) or −/− (C) mouse demonstrates development of marrow cavity in +/+ vertebra is already established *vs.* the c-*fos* −/− osteopetrotic mutant. D, Representative c-*fos* −/− vossicle after implantation and 21 d of PTH administration. TRAP staining reveals numerous TRAP-positive cells and validates rescue of the osteopetrotic phenotype. E, Luciferase imaging of a vossicle implant from a luciferase tagged mouse into an athymic mouse and imaged with a CCD camera at 1 wk to demonstrate the localized luciferase positivity at the implant site (three implants shown). F, Immunohistochemistry for luciferase from a luciferase-tagged vossicle from a mouse treated with PTH for 3 wk. The positive luciferase staining in the osteoblastic cells lining the bony trabeculae verifies the donor origin of these cells. Magnification, ×25 (B–D) or ×200 (F).

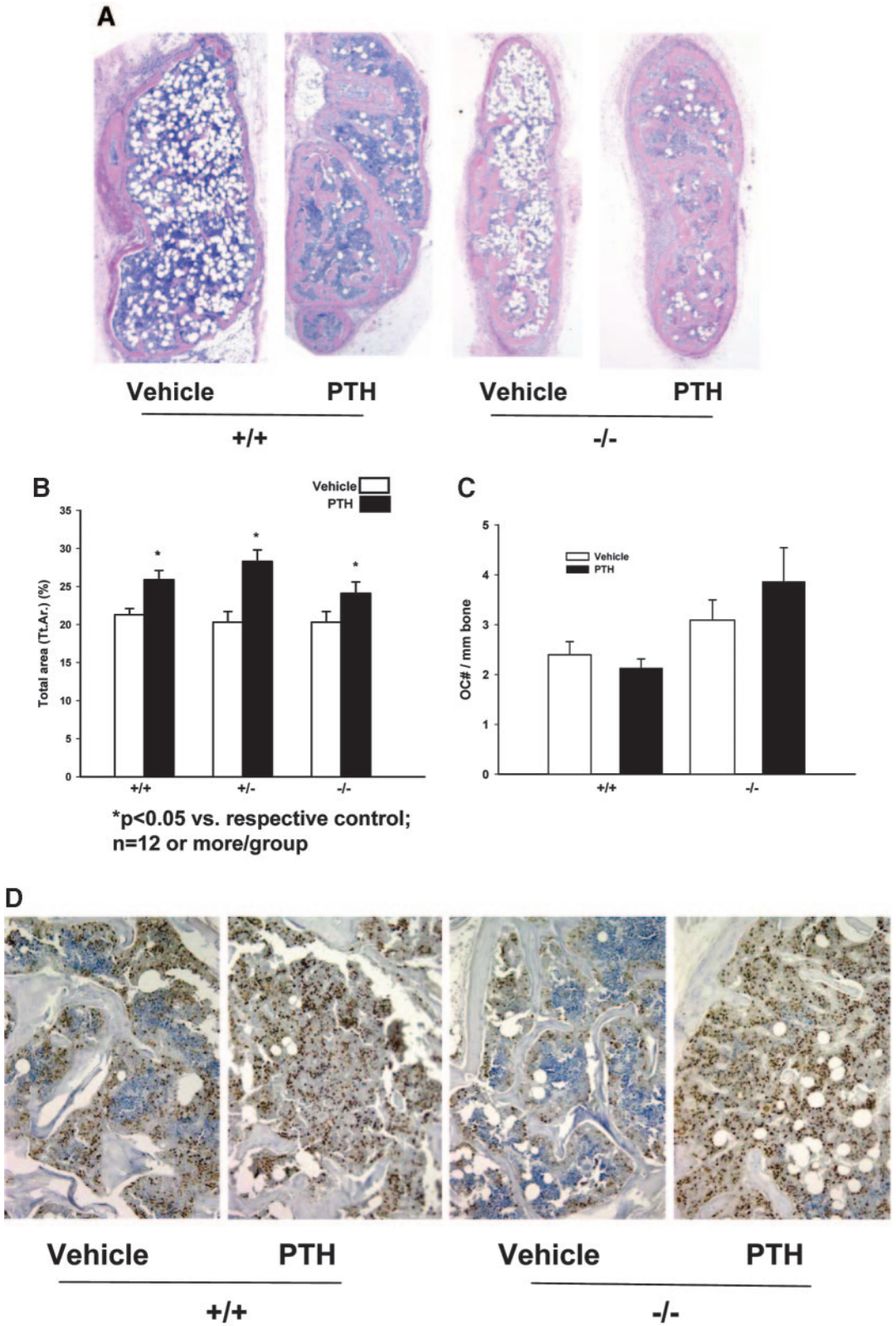

FIG. 4. Vossicles from PTH-treated c-*fos* mutant and wild-type mice. A, Representative H&E-stained c-*fos* +/+ and −/− vossicles from vehicle- and PTH (80 μg/kg·d; 21 d)-treated mice (×20). B, Graph of total bone area (Tt.Ar.) as a percentage of the overall size of vossicles from vehicle- and PTH-treated c-*fos* +/+ and −/− mice (n = 12 or more/group). C, Numbers of osteoclasts per millimeter of bone from vossicles in B (n = 8–9 per group; no significant difference between groups). D, Representative BrdU-stained sections from B demonstrating localized positivity lining the trabecular bone in vehicle-treated mice and a more widespread positivity in the PTH-treated mice from both genotypes (×160).

lining the bony surfaces, whereas with PTH treatment there was increased and a more widespread distribution of BrdU positivity that extended throughout the bone marrow. This suggests that cells in the marrow compartment that is derived from the host are likely to be the important targets of PTH action.

The finding of a rescued anabolic phenotype of PTH on c-*fos* −/− vossicles led us to explore the dependence of PTH on cells of the osteoclast lineage for the anabolic response. Mice with wild-type vossicle implants were treated with OPG, a decoy receptor for receptor activator of nuclear factor κB (RANK) ligand (RANKL), and an inhibitor of osteoclast differentiation. OPG was administered alone or in combination with PTH (Fig. 5). OPG alone did not alter the bone area of vossicles but did significantly block the PTH anabolic response. These data suggest that PTH requires osteoclastic activity for its anabolic response and fits with the lack of response in the intact c-*fos* osteopetrotic mouse. However, because OPG was administered early in the treatment protocol, by the time the mice were killed, there was no difference in the numbers of osteoclasts per millimeter of bone (data not shown). Interestingly, the c-*fos* mutant mice have an arrest in osteoclast differentiation fairly early in osteoclast development. The recruitment of hematopoietic cells to sites of active resorption is the first step in osteoclastogenesis. This has been reported to be at least in part, due to the up-regulation of SDF-1 in stromal cells and its interaction with its receptor, CXCR4. We have previously shown that PTH up-regulates SDF-1 in the mesenchymal compartment of developing ossicles so the impact of disrupting this system by administering blocking agents to inhibit the CXCR4 was determined (31). Figure 6A demonstrates that SDF-1 levels are increased in tibiae of mice administered PTH in an anabolic mode. Interestingly, blocking SDF-1 activity was successful in reducing the anabolic action of PTH in the vossicle model system of wild-type mice (Fig. 6, B and C).

To further identify the osteoclastic stage dependence for this effect, we employed another osteopetrotic model, the c-*src* mutant mice. The c-*src* mutant mice have a defect in the signaling that is necessary for osteoclast formation of a ruffled membrane and adherence to the bone substrate (32). Hence, they have osteoclastic cells present, but they do not function to resorb bone. Two studies were performed with these mice. A regimen similar to what we published with the c-*fos* mutant mice was performed where PTH was administered to intact mutant mice from neonatal d 4–21 (18). The second study used the vossicle model where vertebral bodies from c-*src* mutant and wild-type mice were implanted into athymic hosts and PTH administered over a 3-wk period. Interestingly, in both of these regimens, PTH displayed an anabolic response. Figure 7A demonstrates the microradiographic view of femurs, and Fig. 7B a histologic view of vertebrae from vehicle- and PTH-treated c-*src* wild-type and mutant mice. PTH treatment resulted in increased radiopacity and increased trabecular bone in PTH-treated mice regardless of the c-*src* status. Figure 7, C and D, demonstrate the vossicle model where there is an increase in bone area in all genotypes of c-*src* mice. This suggests that the stage of osteoclast differentiation is critical for anabolic actions of PTH in this model system.

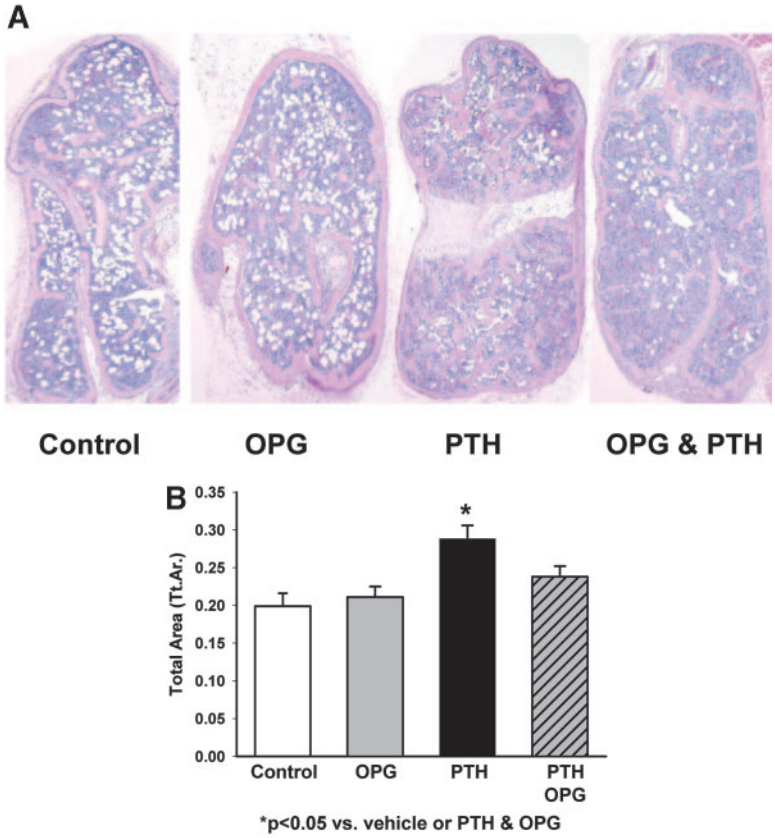

FIG. 5. Vossicles from mice treated with OPG with or without PTH. Vertebrae from wild-type mice were implanted into athymic hosts and mice administered PTH (80 μg/kg·d; 21 d) or OPG (4 mg/kg twice a week for the first 2 wk) or a combination of PTH and OPG. A, Representative H&E-stained vossicles (×25). B, Graph of total bone area (Tt.Ar.) of vossicles from indicated treatment groups (n = 8 control, n = 12 each for OPG, PTH, PTH, and OPG). PTH treatment resulted in an anabolic response, and OPG significantly blocked the anabolic response of PTH.

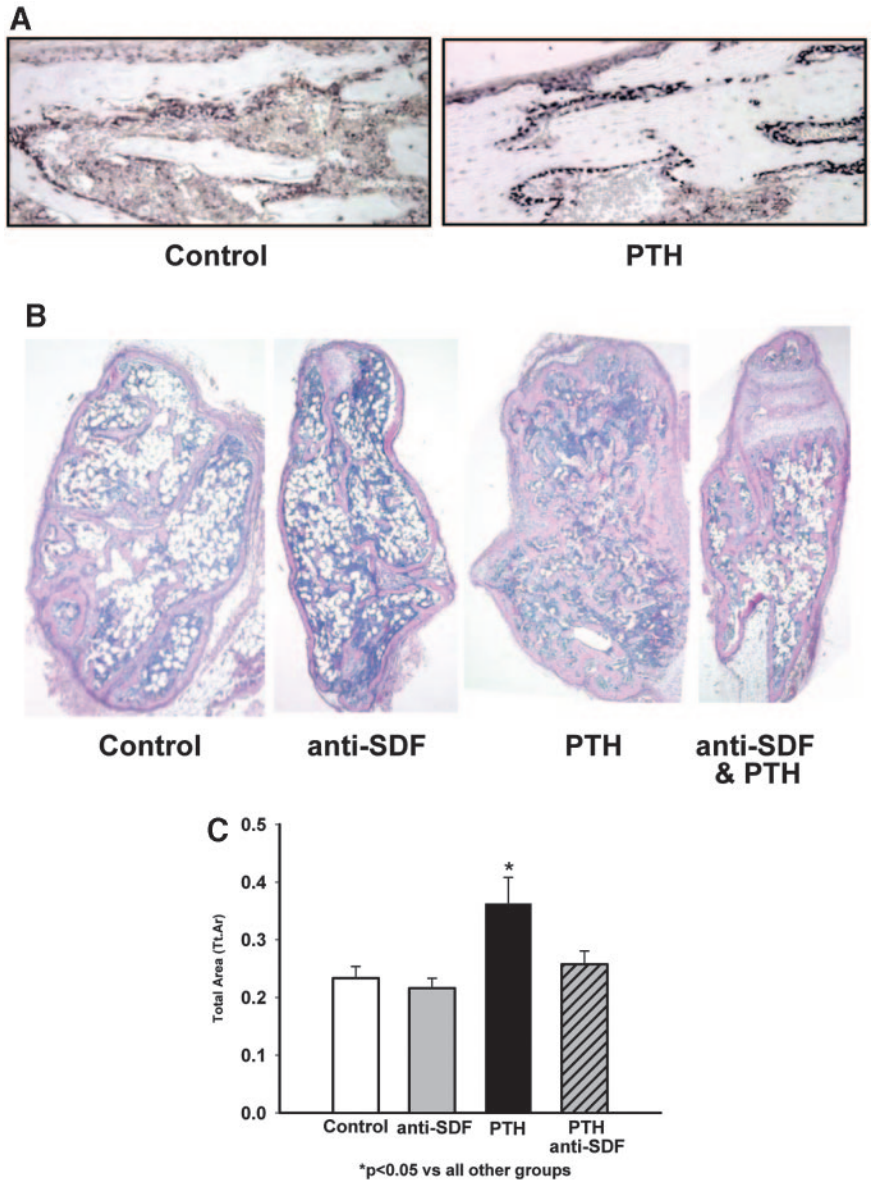

FIG. 6. Impact of blocking SDF-1 on the anabolic action of PTH. A, *in situ* hybridization for SDF-1 in tibiae from mice administered PTH (80 μg/kg) or vehicle (×100) for 3 wk. Positivity for SDF-1 was detected in areas of bone formation in cells lining the trabecular surface with osteoblast-like appearance. SDF-1 positivity was greater in mice treated with PTH. Vertebrae from wild-type mice were implanted into athymic hosts, and mice were treated with anti-CXCR4 blocking peptide designed to inhibit SDF-1 binding to CXCR4 (1 μg/d) and antihuman/mouse SDF-1 IgG antibody (25 μg/d) (group indicated as anti-SDF) with or without PTH (80 μg/kg·d) for 21 d. B, Representative H&E-stained vossicles (×25). C, Graph of total bone area (Tt.Ar.) of vossicles from indicated treatment groups (n = 6 control, 6 anti-SDF, 4 PTH, 8 PTH + anti-SDF). Data are mean ± SEM. PTH treatment resulted in an anabolic response, and inhibition of SDF-1 activity significantly blocked the anabolic response of PTH.

Discussion

The present study was performed to better understand the anabolic actions of PTH and delineate the specific role of c-*fos* as a transcriptional mediator of PTH actions in bone. This work stemmed from our previous work where we found that mice with ablation of the c-*fos* gene did not respond to PTH in an anabolic mode (18). The c-*fos* mutant mice responded to PTH, but in an antianabolic mode where instead of an increase in bone there was actually a reduction in bone area with PTH treatment. These data suggested that c-*fos* gene expression was critical for the anabolic actions of PTH and prompted the dissection of the specific cellular targets of PTH that discriminated the anabolic and antianabolic effects. To do this, *in vitro* approaches and a novel *in vivo* model were used. The *in vitro* studies indicate that the direct actions of PTH on cells of the osteoblast lineage are to inhibit their differentiation and mineralization. This is consistent with the antianabolic response that was found *in vivo* when c-*fos* was ablated. Our laboratory and others have previously presented data that support an inhibition of mineralization by PTH (25, 33). More importantly, it became clear during this investigation that c-*fos* may be an indirect target of PTH anabolic actions via its role in osteoclastogenesis and not via a direct impact in the mesenchymal compartment.

Fos is important in growth, differentiation, transformation, and regulation of specific gene expression, all of which are key events in bone homeostasis (15). During embryogenesis, c-*fos* is expressed in growth regions of fetal bones,

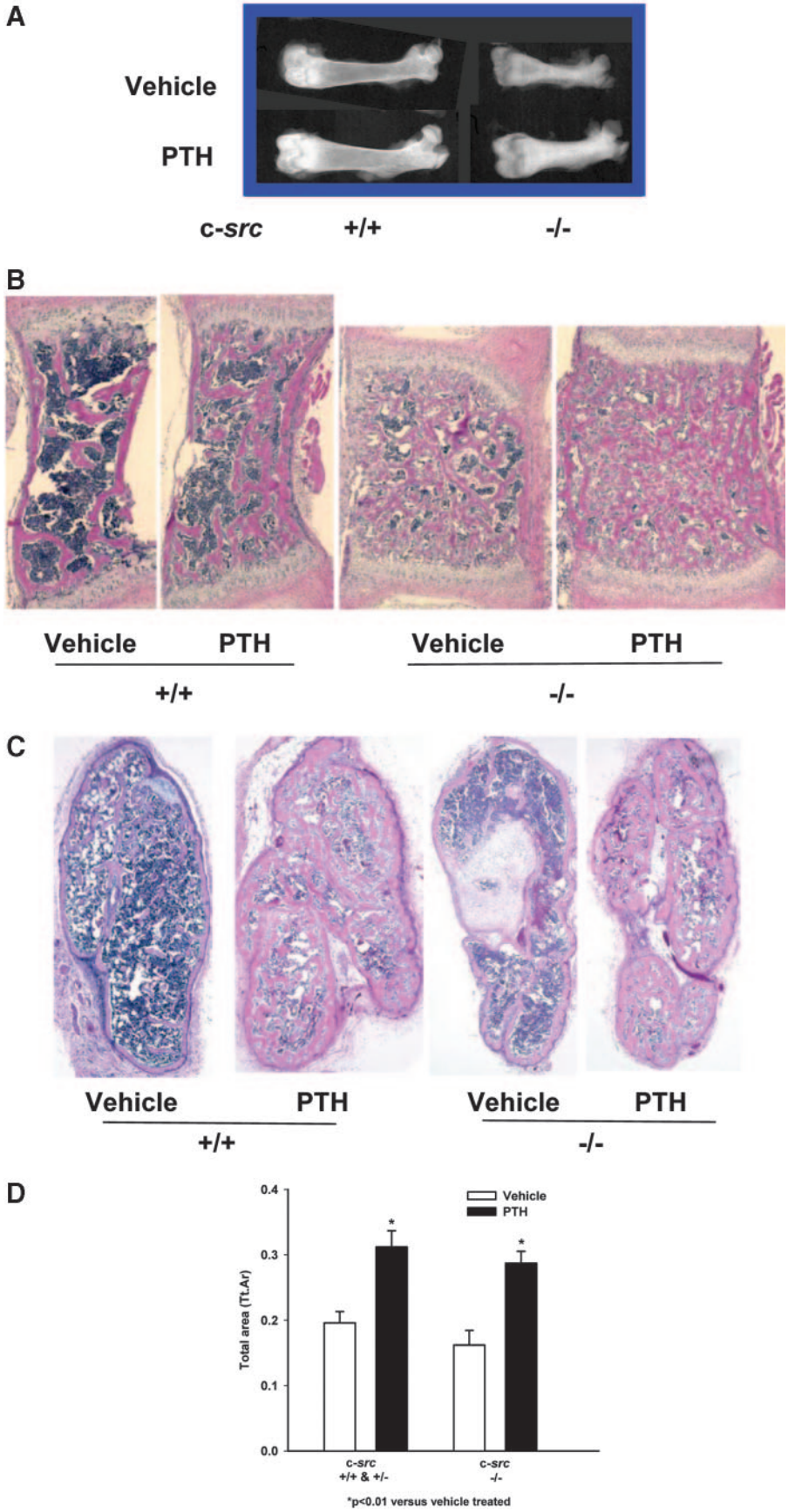

FIG. 7. Impact of *c-src* mutation on anabolic actions of PTH. A and B, Mice from heterozygous *c-src* +/− breedings were administered PTH (50 μg/kg·d) or vehicle from d 4–21 postnatal age. Mice were killed, and microradiography revealed an anabolic PTH response in femurs (A) and an increase in vertebral trabecular bone (B) from both c-*src* +/+ and −/− mice. C, Vertebrae from 4-d-old c-*src* +/+, +/−, and −/− mice were implanted into athymic hosts and PTH (80 μg/kg·d) or vehicle administered for 21 d. Representative H&E stain demonstrates vossicles from PTH-treated groups regardless of genotype respond with an increase in trabecular bone. Note the presence of cartilage in the vehicle c-*src* mutant image, which is a common and random finding and is not included in the bone area determination or osteoclast enumeration. D, Graph of total bone area (Tt.Ar.) of vossicles from PTH-treated c-*src* +/+, +/−, and −/− mice (n = 12 and 11 for c-*src* +/+ and +/− vehicle and PTH, respectively, and n = 7 and 8 for c-*src* −/− vehicle and PTH respectively). An anabolic response to PTH was found regardless of the genotype. Magnification ×2.5 (A), ×30 (B), and ×25 (C).

areas that have active osteoblast proliferation (34). Many studies have suggested that c-*fos* is associated with and is important for cell proliferation (35). However, in the present study, primary osteoblasts of mice with an ablation of c-*fos* had increased cell viability compared with their wild-type counterparts. A previous study found c-*fos*-deficient fibroblasts retain their ability to proliferate *in vitro*, indicating there was no difference in proliferation between genotypes, although they noted a slight increase in c-*fos* −/− cells at d 4 (36). The cell types used were different from ours, but our findings were similar at that time point. The increased cell number at d 8 in the present study suggests an effect on contact inhibition because the cells became confluent between d 5 and 6. It has been proposed that c-*fos* may be important in apoptosis (37). However, in the present study, cells from both genotypes responded similarly to etoposide treatment, which is a known apoptotic agent. Furthermore, cells from c-*fos* mutant mice had increased levels of cyclin D1, a cyclin responsible for G_1 cell cycle progression. Because the cyclin D1 promoter contains an AP-1 site, and we have found JunB to negatively regulate cyclin D1 (29), this suggests that c-Fos may partner with JunB as cells become confluent to restrict their cell cycle progression and in the absence of Fos or JunB that cells may continue their proliferation. Importantly, our studies found only this single difference between c-*fos* mutant and wild-type cells and did not find any differences in the response of the c-*fos* mutant cells to PTH. This suggests that the differences seen in the intact animal (lack of an anabolic response to PTH) are not associated with a direct effect of PTH on osteoblastic cells. Because c-*fos* is an essential mediator of osteoclastogenesis, the impact of cells of the osteoclast lineage was evaluated.

Osteoclastogenesis is a complex process that includes recruitment of cells to the resorptive site, differentiation, multinucleation, and activation (38). Cross talk between osteoclasts and osteoblasts has been discussed for many years, but most of the convincing evidence has centered on osteoblast signaling to osteoclasts via the RANK/RANKL system. Osteoclast signaling to recruit osteoblastic cells to repair the resorptive lacunae has also been discussed, but much of the focus has been on the osteoclast release of growth factors stored in the bone, such as TGFβ, that stimulate osteoblast differentiation or chemotaxis (39). The present study supports a concept of cross talk between osteoclastic cells that are not actively resorbing matrix but are multinucleated cells. To substantiate this, four intervention strategies were investigated. Blocking SDF-1/CXCR4 was performed to inhibit recruitment of osteoclast progenitor cells. SDF-1 is an osteoblast- or endothelial-derived chemokine that directs osteoclast precursors into bone marrow to appropriate sites for differentiation into active osteoclasts (40). Blocking SDF-1 activity via the administration of blocking peptides and/or antibodies to the SDF-1 receptor, chemokine receptor-4 (CXCR4), has been used as a method to block cancer metastasis and decrease osteoclastic activity (23, 24). The same approach was used here to block osteoclast recruitment during PTH administration. The anabolic response to PTH in mice was blocked when SDF-1 activity was inhibited. This suggests that cells recruited to the marrow in response to resorptive stimuli are necessary for the anabolic response to PTH. The BrdU labeling studies revealed the widespread presence of proliferative cells in the bone marrow of PTH-treated mice and support key cellular targets in the marrow. Recent data of Calvi *et al.* (41) demonstrate a role for osteoblasts in regulating the hematopoietic niche. They found that PTH increased expression of the Notch ligand jagged 1 to support an increase in the number of hematopoietic cells. Findings of the present study further suggest that PTH may stimulate osteoblasts to recruit hematopoietic cells that then signal back to osteoblasts to increase bone formation.

The SDF-1 blocking experiments do not restrict the cellular targets to osteoclasts. Hence, OPG studies were performed to block the differentiation of cells along the osteoclast lineage. OPG acts as a decoy receptor that blocks the interaction of RANK and RANKL and hence inhibits osteoclast differentiation (32, 42). Administration of OPG in combination with PTH in the vossicle model was capable of blocking the anabolic response. This further supports the necessity for osteoclastogenesis as a key factor in the anabolic actions of PTH. However, dendritic cells also express RANK, and OPG could conceivably interact with RANK on the surface of dendritic cells and alter PTH responses if a dendritic cell was a relevant target. The expression of c-*fos* is essential for osteoclastogenesis at the point which cells differentiate from macrophages and fuse into multinucleated cells (12, 32). Mice lacking c-*fos* do not have osteoclasts and are osteopetrotic but display increased numbers of macrophages. Data in the intact c-*fos* mutants show that PTH is not anabolic (18), whereas in the vossicle transplants, which contain a host-derived hematopoietic marrow and TRAP-positive multinucleated osteoclastic cells and the anabolic PTH response is rescued, suggest that c-*fos* expression in the marrow is critical for the anabolic response. Furthermore, it suggests that macrophages in abundance in the c-*fos* mutants cannot rescue the PTH response. Finally, data from the c-*src* mutant mice provide evidence that the presence of active resorbing osteoclasts may not be critical for the PTH response. The c-*src* mutant mice lack functional osteoclasts due to a defect in activation associated with cytoskeletal rearrangement and motility (32). These mice present with numerous multinucleated TRAP-positive cells, but these cells fail to form ruffled borders and resorption lacunae (43, 44). The data in the present study where intact c-*src* mutant mice retained the ability to mount an anabolic response to PTH suggest against the necessity for active bone resorption and subsequent release of growth factors from the bone matrix to feedback to osteoblastic cells. Instead, these data implicate cells of the osteoclast lineage at the developmental stage of marrow localization and multinucleation before active bone resorption. We hypothesize that these cells are producing a factor/factors that are signaling to osteoblasts to increase bone formation. Of note, the c-*src* mutant mice have been reported to have an osteoblast phenotype as well as the osteoclast phenotype that supports increased osteoblast activity (45, 46). Data from the vossicle model where osteoblasts are compartmentalized from the hematopoietic cells suggest that this alteration does not play into the effects of PTH because there was no difference in bones from mutant or wild-type mice.

The data in the present study that implicate cells of the osteoclast lineage are particularly intriguing in light of the

recent clinical studies where administration of an antiresorptive bisphosphonate in combination with PTH did not augment the increase in bone volume. Bisphosphonates have been shown to inhibit osteoclast activity at four levels: 1) inhibition of osteoclast recruitment, 2) inhibition of osteoclast adhesion, 3) shortening of osteoclast lifespan, and 4) direct inhibition of osteoclast activity (47). According to the hypothesis presented here, the alteration in recruitment would impact the anabolic action of PTH, but the other actions should not compromise cells that may be key targets for anabolic actions of PTH. Furthermore, studies of combinatorial therapy where the antiresorptive calcitonin was administered in combination with PTH did not prove to augment the anabolic action of PTH (48). In contrast, one study reported that the combination of OPG with PTH did not compromise the increase in bone strength that PTH mediated (49); however, this study was performed in rats and under an estrogen-depleted condition that could have modified the outcome.

Other reports highlight cross talk mechanisms between osteoclasts and osteoblasts (50, 51). Two preliminary studies suggest a juxtacrine interaction between osteoclasts and osteoblasts (52, 53). To our knowledge, the present study is the first to provide data to support the role of osteoclastic cells in the action of an anabolic agent although it has been proposed (54). Recent data support the concept of a stage-dependent impact of osteoclasts on the bone formation response. Pharmaceutical strategies were used to inhibit osteoclast acidification, and the data indicated that resorption could be inhibited at this late stage of osteoclast differentiation without altering bone formation (55). Hence, the data presented here and in conjunction with other studies strongly suggest that cells in the intermediately differentiated population of osteoclasts may be key targets for PTH anabolic action. Interestingly, that cells in the marrow were targets of PTH action was proposed more than 10 years ago, but perhaps because of the focus then on catabolic actions of PTH, little was done to substantiate this work in regards to anabolic actions (56). It is also important to recognize that although the model system used here is not a model of osteoporosis but may be more applicable to clinical scenarios in bone regeneration for local tissue engineering strategies where PTH has also been found to be anabolic (57, 58).

Previous work from our laboratory and others indicate that cells of the osteoblastic lineage are critical for anabolic actions, but our *in vitro* data suggest that they are not the direct targets of PTH action for this anabolic effect. This does not preclude their ability to, while directly inhibiting mineralization, produce factor(s) that signal to cells in the marrow that then direct other osteoblastic cells to form bone. This multilevel regulation may also address the vagaries of an intermittent PTH administration regimen. Data from our ossicle model system point to a role of cells of the osteoblast lineage that are relatively early in their differentiation program and are not lining or terminally differentiated cells (28). Collectively, these current and recent studies suggest that PTH targets stromal cells to signal to cells of the hematopoietic lineage to recruit to sites of remodeling. These cells differentiate and multinucleate, and before adhering to the bone matrix and resorbing bone, they signal either via a paracrine or juxtacrine manner to preosteoblastic cells to differentiate and form bone. The dependence on an osteoclastic cell could also be tested by analyzing the impact of PTH on various other osteopetrotic mutant mouse models such as the PU.1-deficient mice, the M-CSF mutant mice that would lack mature osteoclasts, and the β3 integrin-deficient mice that have osteoclasts but lack functional resorptive activity. The concept presented here has obvious clinical application in the consideration of combination antiresorptive and anabolic agent therapies. The use of antiresorptives that target late stages of osteoclastic activity, such as antiintegrins or proton pump inhibitors, might reduce bone resorption without compromising the support of osteoblastic activity.

Acknowledgments

We thank Dr. Kurt Hankenson for providing the luciferase mice; Erin Ealba, Ana Mattos, and Jason Wang for technical assistance; Daniel Hall for technical support with bioluminescent optical imaging; Chris Strayhorn for histologic/tissue processing support; and T. John Martin for critical reading of the manuscript.

Received March 21, 2005. Accepted July 26, 2005.

Address all correspondence and requests for reprints to: Laurie K. McCauley, D.D.S., Ph.D., Department of Periodontics and Oral Medicine, School of Dentistry, Room 3343, University of Michigan, 1011 North University Avenue, Ann Arbor, Michigan 48109-1078. E-mail: mccauley@umich.edu.

This work was supported by National Institutes of Health Grants DK53904 (to L.K.M.) and DE13701 (to R.S.T.) and by a fellowship from TUBITAK: The scientific and technological research council of Turkey (NATO-A2 to B.D.).

References

1. **Neer RM, Arnaud CD, Zanchetta JR, Prince R, Gaich GA, Reginster JY, Hodsman AB, Eriksen EF, Ish-Shalom S, Genant H, Wang O, Mitlak BH** 2001 Effect of parathyroid hormone (1–34) on fractures and bone mineral density in postmenopausal women with osteoporosis. New Engl J Med 10:1434–1441
2. **Mohan S, Kutilek S, Zhang C, Shen HG, Kodama Y, Srivastava AK, Wergedal JE, Beamer WG, Baylink DJ** 2000 Comparison of bone formation response to parathyroid hormone (1–34), (1–31), and (2–34) in mice. Bone 27:471–478
3. **Rixon RH, Whitfield JF, Gagnon L, Isaacs RJ, Maclean S, Chakravarthy B, Durkin JP, Neugebauer W, Ross V, Sung W, Willick GE** 1994 Parathyroid hormone fragments may stimulate bone growth in ovariectomized rats by activating adenylyl cyclase. J Bone Miner Res 9:1179–1189
4. **Jilka RL, Weinstein RS, Bellido T, Roberson P, Parfitt AM, Manolagas SC** 1999 Increased bone formation by prevention of osteoblast apoptosis with parathyroid hormone. J Clin Invest 104:439–446
5. **Bellido T, Ali AA, Plotkin LI, Fu Q, Gubrij I, Roberson PK, Weinstein RS, O'Brien CA, Manolagas SC, Jilka RL** 2003 Proteasomal degradation of Runx2 shortens parathyroid hormone-induced anti-apoptotic signaling in osteoblasts. A putative explanation for why intermittent administration is needed for bone anabolism. J Biol Chem 278:50259–50272
6. **Black DM, Greenspan SL, Ensrud KE, Palermo L, McGowan JA, Lang TF, Garnero P, Bouxsein ML, Bilezikian JP, Rosen CJ** 2003 The effects of parathyroid hormone and alendronate alone or in combination in postmenopausal osteoporosis. New Engl J Med 25:1207–1215
7. **Finkelstein JS, Hayes A, Hunzelman JL, Wyland JJ, Lee H, Neer RM** 2003 The effects of parathyroid hormone, alendronate, or both in men with osteoporosis. New Engl J Med 25:1216–1226
8. **Delmas PD, Vergnaud P, Arlot ME, Pastoureau P, Meunier PJ, Nilssen MH** 1995 The anabolic effect of human PTH (1–34) on bone formation is blunted when bone resorption is inhibited by the bisphosphonate tiludronate–is activated resorption a prerequisite for the *in vivo* effect of PTH on formation in a remodeling system? Bone 16:603–610
9. **Clohisy JC, Scott DK, Brakenhoff KD, Quinn CO, Partridge NC** 1992 Parathyroid hormone induces c-*fos* and c-*jun* messenger RNA in rat osteoblastic cells. Mol Endocrinol 6:1834–1842
10. **McCauley LK, Koh AJ, Beecher CA, Rosol TJ** 1997 The proto-oncogene c-*fos* is transcriptionally regulated by PTH and PTHrP in a cAMP-dependent manner in osteoblastic cells. Endocrinology 138:5427–5433
11. **Finkel MP, Biskis BO, Jinkins PB** 1966 Virus induction of osteosarcomas in mice. Science 151:698–701

12. **Grigoriadis AE, Wang ZQ, Cecchini MG, Hofstetter W, Felix R, Fleisch HA, Wagner EF** 1994 c-Fos: a key regulator of osteoclast-macrophage lineage determination and bone remodeling. Science 266:443–448
13. **Tolar J, Teitelbaum SL, Orchard PJ** 2004 Osteopetrosis. New Engl J Med 30:2839–2849
14. **Wang ZQ, Grigoriadis AE, Mohle-Steinlein U, Wagner EF** 1991 A novel target cell for c-*fos* induced oncogenesis: development of chrondrogenic tumours in embryonic stem cell chimeras. EMBO J 10:2437–2450
15. **Grigoriadis AE, Wang ZQ, Wagner EF** 1995 *Fos* and bone cell development: lessons from a nuclear oncogene. Trends Genet 11:436–441
16. **Wang ZQ, Ovitt C, Grigoriadis AE, Mohle-Steinlein U, Ruther U, Wagner EF**1992 Bone and haematopoietic defects in mice lacking c-*fos*. Nature 360: 741–745
17. **Johnson RS, Spiegelman BM, Papaioannou V** 1992 Pleiotropic effects of a null mutation in the c-*fos* proto-oncogene. Cell 71:577–586
18. **Demiralp B, Chen H, Koh-Paige AJ, Keller ET, McCauley LK** 2002 Anabolic effects of parathyroid hormone during endochondral bone growth are dependent on c-*fos*. Endocrinology 143:4038–4047
19. **Soriano P, Montgomery C, Geske R, Bradley A** 1991 Targeted disruption of the c-*src* proto-oncogene leads to osteopetrosis in mice. Cell 64:693–702
20. **Yull FE, Wei H, Jansen ED, Everhart MB, Sadikot RT, Christman JW, Blackwell T** 2003 Bioluminescent detection of endotoxin effects on HIV-1 LTR-driven transcription *in vivo*. J Histochem Cytochem 51:741–749
21. **Kalikin LM, Schneider A, Thakur MA, Fridman Y, Griffin LB, Dunn RL, Rosol TJ, Shah RB, Rehemtulla A, McCauley LK, Pienta KJ** 2003 In vivo visualization of metastatic prostate cancer and quantitation of disease progression in immunocompromised mice. Cancer Biol Ther 2:656–660
22. **Tamamura H, Omagari A, Hiramatsu K, Kanamoto T, Xu YN, Kodama E, Matsuoka M, Hattori T, Yamamoto N, Nakashima H, Otaka A, Fujii N** 2001 Development specific CXCR4 inhibitors possessing high selectivity indexes as well as complete stability in serum based on an anti-HIV peptide T140. Bioorg Med Chem Lett 11:1897–1902
23. **Liang Z, Wu T, Lou H, Yu X, Taichman RS, Lau SK, Nie S, Umbreit J, Shim H** 2004 Inhibition of breast cancer metastasis by selective synthetic polypeptide against CXCR4. Cancer Research 64:4302–4308
24. **Sun YX, Schneider A, Jung Y, Wang J, Dai J, Wang J, Cook K, Osman NI, Koh-Paige AJ, Shim H, Pienta KJ, Keller ET, McCauley LK, Taichman RS** 2005 Skeletal localization and neutralization of the SDF-1(CXCL12)/CXCR4 axis blocks prostate cancer metastasis and growth in osseous sites *in vivo*. J Bone Miner Res 20:318–329
25. **Koh AJ, Beecher CA, Rosol TJ, McCauley LK** 1999 Cyclic AMP activation in osteoblastic cells: effects on PTH-1 receptors and osteoblastic differentiation *in vitro*. Endocrinology 140:3154–3162
26. **Chen C, Koh AJ, Datta NS, Zhang J, Keller ET, Xiao G, Franceschi RT, D'Silva N, McCauley LK** 2004 Impact of the mitogen-activated protein kinase pathway on parathyroid hormone-related protein actions in osteoblasts. J Biol Chem 279:29121–29129
27. **McCauley LK, Koh AJ, Beecher CA, Cui Y, Decker JD, Francheschi RT** 1995 Effects of differentiation and transforming growth factor β on PTH/PTHrP receptor mRNA levels in MC3T3–E1 cells. J Bone Miner Res 10:1243–1255
28. **Pettway GJ, Schneider A, Koh AJ, Widjaja E, Morris MD, Meganck JA, Goldstein SA, McCauley LK** 2005 Anabolic actions of PTH (1–34): use of a novel tissue engineering model to investigate temporal effects on bone. Bone 36:959–970
29. **Datta NS, Chen C, Berry JE, McCauley LK** 2005 PTHrP signaling targets cyclin D1 and induces osteoblastic cell growth arrest. J Bone Miner Res 20:1051–1064
30. **Schneider A, Taboas J, McCauley LK, Krebsbach PH** 2003 Skeletal homeostasis in tissue-engineered bone. J Orthop Res 21:859–864
31. **Jung Y, Wang J, Schneider A, Sun YX, Koh-Paige AJ, Osman NI, McCauley LK, Taichman RS** 2005 Regulation of SDF-1 (CXCL12) Production by osteoblasts in the hematopoietic microenvironment and a possible mechanisms for stem cell homing. J Bone Miner Res 19:S389
32. **Boyle WJ, Simonet WS, Lacey DL** 2003 Osteoclast differentiation and activation. Nature 423:337–342
33. **Bellows CG, Ishida H, Aubin JE, Heersche JNM** 1990 Parathyroid hormone reversibly suppresses the differentiation of osteoprogenitor cells into functional osteoblasts. Endocrinology 127:3111–3116
34. **Dony C, Gruss P** 1987 Proto-oncogene c-*fos* expression in growth regions of fetal bone and mesodermal web tissue. Nature 328:711–714
35. **Angel P, Karin M** 1991 The role of Jun, Fos, and the AP-1 complex in cell proliferation and transformation. Biochim Biophys Acta 1072:129–157
36. **Hu E, Mueller E, Olivero S, Papaioannou V, Johnson R, Spiegelman BM** 1994 Targeted disruption of the c-*fos* gene demonstrates c-*fos*-dependent and -independent pathways for gene expression stimulated by growth factors or oncogenes. EMBO J 13:3094–3103
37. **Smeyne RJ, Vendrell M, Hayward M, Baker S, Miao GG, Schilling K, Robertson LM, Curran T, Morgan JI** 1993 Continuous c-*fos* expression precedes programmed cell death *in vivo*. Nature 363:166–169
38. **Teitelbaum SL** 2000 Bone resorption by osteoclasts. Science 289:1504–1508
39. **Centrella M, Horowitz MC, Wozney JM, McCarthy TL** 1994 Transforming growth factor-β gene family members and bone. Endocr Rev 15:27–39
40. **Yu X, Huang Y, Collin-Osdoby P, Osdoby P** 2003 Stromal cell-derived factor-1 (SDF-1) recruits osteoclast precursors by inducing chemotaxis, matrix metalloproteinase-9 (MMP-9) activity, and collagen transmigration. J Bone Miner Res 18:1404–1418
41. **Calvi LM, Adams GB, Welbrecht KW, Weber JM, Olson DP, Knight MC, Martin RP, Schipani E, Divieti P, Bringhurst FR, Milner LA, Kronenberg HM, Scadden DT** 2003 Osteoblastic cells regulate the haematopoietic stem cell niche. Nature 425:841–846
42. **Simonet WS, Lacey DL, Dunstan CR, Kelley M, Chang MS, Luthy R, Nguyen HQ, Wooden S, Bennett L, Boone T, Shimamoto G, DeRose M, Elliott R, Colombero A, Tan HL, Trail G, Sullivan J, Davy E, Bucay N, Renshaw-Gegg L, Hughes TM, Hill D, Pattison W, Campbell P, Sander S, Van G, Tarpley J, Derby P, Lee R, Boyle WJ**1997 Osteoprotegerin: a novel secreted protein involved in the regulation of bone density. Cell 89:159–161
43. **Lowe C, Yondea T, Boyce BF, Chen H, Mundy GR, Soriano P** 1993 Osteopetrosis in Src-deficient mice is due to an autonomous defect of osteoclasts. Proc Natl Acad Sci USA 90:4485–4489
44. **Boyce B, Yoneda T, Lowe C, Soriano P, Mundy GR** 1992 Requirement of pp60 c-*src* expression for osteoclasts to form ruffled borders and resorb bone in mice. J Clin Invest 90:1622–1627
45. **Marzia M, Sims NA, Voit S, Migliaccio S, Taranta A, Bernardini S, Faraggiana T, Yoneda T, Mundy GR, Boyce BF, Baron R, Teti A** 2000 Decreased c-*src* expression enhances osteoblast differentiation and bone formation. J Cell Biol 151:311–320
46. **Zaidi SK, Sullivan AJ, Medina R, Ito Y, Van Wijnen AJ, Stein JL, Lian JB, Stein GS** 2004 Tyrosine phosphorylation controls Runx2-mediated subnuclear targeting of YAP to repress transcription. EMBO J 23:790–799
47. **Fleisch H, Reszka A, Rodan G, Rogers M** 2002 Bisphosphonates: mechanisms of action. In: Bilezikian JP, Raisz LG, Rodan G, eds. Principles of bone biology. San Diego: Academic Press; 1361–1385
48. **Hodsman AB, Fraher LJ, Watson PH, Ostbye T, Stitt LW, Adachi JD, Taves DH, Drost D** 1997 A randomized controlled trial to compare the efficacy of cyclical parathyroid hormone versus cyclical parathyroid hormone and sequential calcitonin to improve bone mass in postmenopausal women with osteoporosis. J Clin Endocrinal Metab 82:620–628
49. **Kostenuik PJ, Capparelli C, Morony S, Adamu S, Shimamoto G, Shen V, Lacey DL, Dunstan CR** 2001 OPG and PTH-(1–34) have additive effects on bone density and mechanical strength in osteopenic ovariectomized rats. Endocrinology 142:4295–4304
50. **Zhu J, Emerson SG** 2004 A new bone to pick: osteoblasts and the haematopoietic stem-cell niche. Bioessays 26:595–599
51. **Taichman RS** 2005 Blood and bone: two tissues whose fates are intertwined to create the hematopoietic stem cell niche. Blood 105:2631–2639
52. **Phan T, Han R, Davey T, Smut V, Zheng MH, Xu J** 2004 Identification and functional characterization of a novel osteoclast-derived osteoblastic factor (ODOF). J Bone Miner Res 19:S37
53. **Zhao C, Irie N, Shimoda K, Miyamoto T, Nishiwaki T, Ishikawa H, Suda T** 2004 Bidirectional signaling by Ephrinb2-EphB4 coordinates osteoclast and osteoblast functions to enhance bone formation. J Bone Miner Res 19:S14
54. **Martin TJ** 2004 Does bone resorption inhibition affect the anabolic response to parathryoid hormone? Trends Endocrinol Metab 15:49–50
55. **Karsdal MA, Henriksen K, Sorensen MG, Gram J, Schaller S, Dziegiel MH, Heegaard AM, Christophersen P, Martin TJ, Christiansen C, Bollerslev J** 2005 Acidification of the osteoclastic resorption compartment provides insight into the coupling of bone formation to bone resorption. Am J Pathol 166:467–476
56. **Rouleau MF, Mitchell J, Goltzman D**1998 *In vivo* distribution of parathyroid hormone receptors in bone: evidence that a predominant osseous target cell is not the mature osteoblast. Endocrinology 123:187–191
57. **Andreassen TT, Willick GE, Morley P, Whitfield JF** 2004 Treatment with parathyroid hormone hPTH(1–34), hPTH(1–31), and monocyclic hPTH(1–31) enhances fracture strength and callus amount after withdrawal fracture strength and callus mechanical quality continue to increase. Calcif Tissue Int 74:351–356
58. **Chen H, Frankenberg L, Goldstein SA, McCauley LK** 2003 The combination of local and systemic PTH enhances fracture healing. Clin Orthop Relat Res 416:291–302

***Endocrinology* is published monthly by The Endocrine Society (http://www.endo-society.org), the foremost professional society serving the endocrine community.**